Annals of Biomedical Engineering, Vol. 41, No. 10, October 2013 (© 2013) pp. 2193–2205
DOI: 10.1007/s10439-013-0803-9

Transport Limitations of Nitric Oxide Inhibition of Platelet Aggregation under Flow

J. L. SYLMAN,[1] S. M. LANTVIT,[2] M. C. VEDEPO,[1] M. M. REYNOLDS,[2,3] and K. B. NEEVES[1,4]

[1]Department of Chemical and Biological Engineering, Colorado School of Mines, 1600 Illinois Street, Golden, CO 80401, USA; [2]Department of Chemistry, Colorado State University, Ft. Collins, CO, USA; [3]School of Biomedical Engineering, Colorado State University, Ft. Collins, CO, USA; and [4]Department of Pediatrics, University of Colorado Denver, Aurora, CO, USA

(*Received 14 December 2012; accepted 26 March 2013; published online 6 April 2013*)

Associate Editor Sriram Neelamegham oversaw the review of this article.

Abstract—Nitric oxide (NO) inhibits platelet aggregation at and near the site of a vascular injury by upregulation of cyclic guanosine monophosphate, which reduces the dimerization of the integrin $\alpha_{IIb}\beta_3$. The magnitude of NO flux from the vessel wall and the NO concentration that is necessary to inhibit platelet aggregation under physiological flow conditions is unknown. In this study, a NO releasing polymer, diazeniumdiolated dibutylhexanediamine, was integrated into a microfluidic flow assay to determine the relationship between NO wall flux and collagen mediated platelet adhesion, activation and aggregation. A NO flux equal to or greater than 2.5×10^{-10} mol cm^{-2} min^{-1} was found to abrogate aggregation, but not initial platelet adhesion, on collagen at 200 and 500 s^{-1} as effectively as the $\alpha_{IIb}\beta_3$ antagonist abciximab. The dynamic range of NO fluxes found to induce measurable inhibition of platelet aggregation spanned from 0.33×10^{-10} to 2.5×10^{-10} mol cm^{-2} min^{-1} at 200–500 s^{-1}. These fluxes correspond to near-wall NO concentrations of 3–90 nM based on a computational model of NO transport. The model predicts that NO concentration in the platelet rich layer near the wall is kinetically limited, while NO penetration into the lumen is mass transfer limited.

Keywords—Biotransport, Endothelium, Hemostasis, Thrombosis.

INTRODUCTION

Endothelial cell derived inhibitors of platelet activation include prostacylins, ADPases, and nitric oxide (NO). NO is a free radical released by the endothelium where it is generated by endothelial nitric oxide synthase (eNOS). Penetration of NO into the lumen is limited by elimination mechanisms that include oxidation and reaction with hemoglobin found in red blood cells (RBC).[13] However, because platelets are concentrated near the vessel wall in a RBC free zone, high concentrations of NO exist that are capable of inhibiting platelet activation.[13] NO passively diffuses through the platelet membrane activating the intracellular receptor soluble guanylyl cyclase (sGC), promoting upregulation of cyclic guanosine monophosphate (cGMP).[5,26] Escalated levels of cGMP activate protein kinase G (PKG), which mediates the NO signaling.[18] PKG directly diminishes platelet reactivity by phosphorylating crucial proteins involved in platelet activation including inositol-1,4,5-triphosphate and receptor associated cGMP kinase substrate, known sources of calcium which provide a favorable environment for platelet activation.[1,18] NO causes platelet agonists such as ADP and thromboxane A_2 to be less potent resulting in reduced integrin dimerization (e.g., $\alpha_{IIb}\beta_3$ and $\alpha_2\beta_1$ in platelets), thereby reducing platelet activation and aggregation.[22] However, the integrity of the receptors glycoprotein VI (GPVI) and glycoprotein (GPIb) are thought to be maintained in the presence of NO because they are constitutively active, and thus can promote initial adhesion onto collagen and VWF, respectively.[21,22]

In vitro studies of platelet function under flow show diminished adhesion, aggregation and spreading in the presence of NO or NO analogs. There is a dose-dependent increase in platelet accumulation downstream from endothelial cells exposed to inhibitors of NO production.[7] Similarly, addition of the NO analog S-nitrosoglutathione to whole blood inhibits VWF-mediated platelet adhesion and spreading through regulation of $\alpha_{IIb}\beta_3$ at 1000 s^{-1}.[21] In this study, NO donor was added directly into the blood prior to a flow assay, and therefore was mixed homogeneously

Address correspondence to K. B. Neeves, Department of Chemical and Biological Engineering, Colorado School of Mines, 1600 Illinois Street, Golden, CO 80401, USA. Electronic mail: kneeves@mines.edu

throughout the blood, rather than concentrated near the wall as expected *in vivo*. Alternatively, NO prepared as a 3.0% (vol/vol) solution in helium-deoxygenated saline has been introduced at the site of platelet adhesion through a porous membrane onto which the extracellular matrix was present and exposed to blood flowing at shear rates of 300–1800 s^{-1}.[7] Another approach reported the introduction of NO gas through a semipermeable membrane underneath adsorbed collagen or fibrinogen. Here, washed platelets were perfused over the surface at 250 and 750 s^{-1} with NO surface concentrations estimated as 0.02–0.15 nM. A surface concentration of ~0.09 nM was found to completely inhibit platelet deposition at all conditions.[20] However, in the absence of RBC, the concentration of platelets near the wall is much lower than would be found in whole blood (due to margination) and NO will not be eliminated by reaction with hemoglobin. There are no studies, that we are aware of, which have measured platelet function at a known NO wall flux using whole blood.

NO secretion from endothelial cells is shear stress dependent with increasing shear stress leading to increased NO production.[11,14] Experiments conducted with cultured bovine aortic endothelial cells suggest a linear relationship between the shear stress and NO flux over the range of 2–10 dyn cm^{-2}.[11] Others have measured the time averaged nitrate/nitrite concentrations from cultured human umbilical vein endothelial cells and find a non-linear two phase relationship between NO production and shear stress—the initial phase dependent on the rate of the change of shear stress and the sustained NO release dependent on the magnitude of the shear stress.[14]

The relationship between shear stress, NO flux and NO transport has been estimated in several computational models.[4,8,19,25,29] Vaughn *et al*. incorporated the reaction with hemoglobin and a reaction-diffusion model of a 50 μm radius arteriole with a NO wall flux of 3.2×10^{-10} mol cm^{-2} min^{-1}.[29] The NO reaction rate constant with RBC was varied between 15 and 1280 s^{-1}. Convective transport was assumed negligible due to relatively fast reaction of NO with RBC. The NO concentration in the vessel varied from 0 to 250 nM and was a strong function of the size of the RBC free layer and the reaction rate constant with blood. A rate constant of 15 s^{-1} gave a NO concentration of 250 nM, which has been reported to be the effective half maximal concentration to activate its main receptor soluble guanylyl cylase.[26] Fadel *et al*.[8] modeled the combined convection, diffusion, and auto-oxidation reaction and linearly related NO production to the wall shear stress. They found that the concentration at the wall is determined by a competition between shear stress dependent production of NO and enhanced removal by convective transport. The NO wall concentration within their computational domain (height of 750 μm and length of 5 cm) varied from 190 to 1100 nM (shear stress range of 0.1–20 dyn cm^{-2}) in the absence of NO elimination with hemoglobin. A finite boundary layer was obtained at shear rates greater than 600 s^{-1} of approximately 100–150 μm, while at 10 s^{-1}, the boundary layer did not completely develop within the length of the chamber.[8] Smith *et al*.[25] reported a model that includes NO elimination by RBC at a rate constant of ~30 s^{-1} and convection with a constant NO flux of 2.0×10^{-11} mol cm^{-2} s^{-1}. They found that the RBC reaction had no effect on NO penetration and found a near wall concentration ranging from 1 to 100 nM. Whether NO penetration into the lumen of a vessel is transport or kinetically limited in these models depends, in part, on the rate constant of NO with blood. This rate constant varies widely in the literature (15–6500 s^{-1}).[27] In addition to elimination with hemoglobin, this lumped reaction rate is thought to represent several transport resistances including the RBC-free layer, packing of hemoglobin in RBCs and external diffusion limitations, many of which remain unknown.

The objective of this study was to measure the relationship between NO wall flux, shear rate and inhibition of platelet aggregation. We decoupled shear rate and NO flux by incorporating NO releasing polymers with known NO fluxes into a microfluidic flow assay. In the experiments, we measured the effect of NO flux on collagen mediated platelet adhesion and aggregation in thrombin inhibited whole blood. The dynamic range of NO flux that inhibited platelet aggregation was determined for shear rates of 200, 500, and 1000 s^{-1}. A computational model of NO transport within the microfluidic device was used to estimate the near-wall NO concentration and to identify the rate limiting transport mechanisms. We explored a range of first order rate constants of NO with blood to determine the rate-limiting step of NO transport. The implications of these transport limitations were then applied to models where the loss of endothelial cells was simulated for various sized injuries.

MATERIALS AND METHODS

Materials

Type I equine tendon insoluble collagen was obtained from Chrono-log Corporation (Havertown, PA, USA). 3,3′-Pacific Blue anti-human CD41 used to label platelets was purchased from BioLegend (San Diego, CA, USA). Cy5 Annexin V used to label phosphatidylserine (PS) was obtained from BD

Biosciences (San Diego, CA, USA). Abciximab, an $\alpha_{IIb}\beta_3$ antagonist (ReoPro, Eli Lilly, Indianapolis, IN, USA), was obtained from University of Colorado Hospital pharmacy. Phe-Pro-Arg-chloromethylketone (PPACK) was obtained from Haematologic Technologies Inc. (Essex Junction, VT, USA). Diazeniumdiolated dibutylhexanediamine (DBHD/N_2O_2) was prepared as previously reported.[3] Potassium tetrakis (4-chlorophenyl) borate (KTpC1PB) was obtained from TCI America (Portland, OR, USA). Mallinckrodt tetrahydrofuran (THF) was purchased from Fisher Scientific (Phillipsburg, NJ, USA). High molecular weight poly(vinyl chloride) (PVC) was obtained from Sigma Aldrich (St. Louis, MO, USA). Plasticizer bis(2-ethylhexyl) sebacate (DOS) was procured from Acros (Springfield, NJ, USA). Phosphate buffered saline (PBS, composed of 137 mM NaCl, 2.7 mM KCl, 10 mM $Na_2HPO_4{\cdot}2\ H_2O$, 2 mM KH_2PO_4, pH 7.4), HEPES buffered saline (HBS, composed of 1 M HEPES, pH 7.2), 10× Binding Buffer (Composed of 0.1 M HEPES, 1.4 M NaCl, 25 mM $CaCl_2$, pH 7.4) and Tyrode's buffer (Composed of 129 mM NaCl, 20 mM HEPES, 12 mM $NaHCO_3$, 2.9 mM KCl, 1.9 mM $MgCl_2$, 0.34 mM $Na_2HPO_4{\cdot}12\ H_2O$, pH 7.3) were made in-house. Microfluidic channels were molded with polydimethylsiloxane (PDMS), which was obtained from Sylgard 184 (Dow Corning, Midland, MI, USA).

Preparation of Collagen Coated NO Releasing Polymer Films

Briefly, glass slides were coated in NO releasing polymer films doped with various concentrations of NO donor (DBHD/N_2O_2) and a top coat. The fluxes of each film preparation were measured using a Sievers chemiluminescence NO Analyzer® NOA, model 280 (GE, Boulder, CO, USA) as previously described[24] (see Supplementary Material for details on preparation and characterization of films). Collagen patterning was performed on all the NO releasing polymer films. A positive control with no polymer coating was also included to measure the effects, if any, of the polymer film on platelet accumulation. The uncoated control was a glass slide made hydrophobic *via* functionalization with octadecyltrichlorosilane (OTS).[31] Type I equine tendon insoluble collagen (Chrono-Log, Havertown, PA, USA) was diluted with 1× PBS to achieve a concentration of 100 μg mL^{-1}. All slides were placed in FAST frame multislide plate containing incubation chambers (Whatman, GE Healthcare Sciences) and incubated with 100 μL of collagen for 1 h. The polymer preparations were not clamped down within the FAST frame to avoid tearing the films, and instead 100 g of weight were placed over the incubation chambers atop the polymer slides. Following incubation, the collagen solution was removed using soft-tip transfer pipettes and each slide was rinsed three times with 1× PBS, washed thoroughly with deionized water and dried. 5 mm × 5 mm squares of collagen were patterned specifically onto the bottom center half of the slide (Suppl. Fig. 1).

Blood Collection and Treatment

All blood collection was performed in accordance with the Declaration of Helsinki and under the University of Colorado, Boulder Institutional Review Board approval. Human whole blood was obtained from donors through venipuncture. All donors had not consumed alcohol for 48 h before, nor taken any prescription or over-the-counter drugs during the 10 days prior. Five milliliters of whole blood required for the microfluidic assay were collected into a syringe containing 75 mM PPACK. The blood was then incubated for 10 min with Pacific Blue anti-human CD41 (platelet label) at 1:100 in the absence or presence of 100 μg mL^{-1} abciximab.

Whole Blood Flow Assay over NO Releasing Polymer Films

Polydimethylsiloxane (PDMS) microfluidic devices, containing four channels with a width of 500 μm and height of 50 μm, were used to simultaneously perfuse whole blood over each surface preparation using previously reported procedures.[10] Fluid was drawn through the microfluidic channels using a syringe pump (PHD 2000, Harvard Apparatus). Outlet channels were connected to a 250, 500 μL or 1 mL syringe. The syringes were placed in the same syringe pump and fluid was withdrawn at 12.5 μL min^{-1}, yielding shear rates of 200, 500 and 1000 s^{-1}. Whole blood was perfused through the device for 5 min at room temperature.

Image Analysis of Platelet Accumulation in Flow Assay

Immediately following the perfusion of the whole blood, HBS containing 2 mM $MgCl_2$ and 2 mM $CaCl_2$ was perfused through the device for 2 min to rinse out the blood. Thrombi were then fixed with 2% glutaraldehyde in HBS for 2 min. Annexin V diluted 1:20 in 1× binding buffer was perfused through the device for 3 min and then the slide was rinsed with deionized water for 2 min. Coverslips were affixed to the slides using Permount medium (Cat # 50-277-97, Fisher Scientific). Platelet accumulation was imaged by confocal microscopy (Olympus Fluoview FV10i) using excitation/emission wavelengths of 488 nm/521 nm for

the anti-CD41 antibody and 630 nm/670 nm for Annexin V. Using a 60× objective (NA = 0.95), ten areas (210 μm × 210 μm) were imaged 1, 1.5, 2, 2.5, and 3 mm downstream the start of the collagen patch. Thrombus heights were attained using the z-stack function on the confocal microscope. The Otsu method was used to threshold the image in ImageJ (NIH, Bethesda, MD). The average platelet aggregate size was calculated from the binary images using the Particle Analyzer function in ImageJ.

Statistical Procedures

Data are presented as a mean ± the standard error mean of 3–4 donors for each experimental condition. Control polymers were compared to the NO releasing polymers and OTS modified glass surface using a Mann–Whitney U-test. For the platelet aggregate heights and areas, significance within each shear rate was determined by a one-way ANOVA test and *post hoc* Tukey test was used to determine the critical NO flux defined as the flux required to be statistically similar to the abciximab condition. A p value of less than 0.05 was considered a statistically significant difference for all tests. All calculations were conducted using Prism 5.

Computational Model of NO Transport

In order to estimate the NO concentration distribution in the experiment, we developed a model of NO transport from the wall at a constant flux flowing into a fluid where the NO can react with oxygen and hemoglobin. The details of the conservation and constitutive equations used in the model, as well as the grid and solver details can be found in the Supplementary Material and Suppl. Fig. 2. Briefly, the steady-state solute conservation equation was solved in a computational domain with the exact dimensions of the microfluidic assay described above. NO was subject to elimination by second-order reaction with oxygen (k_{O2}) and first order reaction with blood (k_B) that represents elimination by hemoglobin in RBC and the associated mass transfer barriers. A commercial finite element method software (COMSOL) was used to solve the conservation equations. The computational domain was divided into subdomains; (i) a platelet rich layer (PRL) near the channel wall that has a thickness of ~3 μm absent of RBC where NO is eliminated by oxidation, and (ii) a bulk domain consisting of RBC where NO is eliminated by oxidation and reaction with blood. This model was extended to simulate an injury where NO was not released from a 100 μm section of the wall in order to estimate the axial transport of NO near an injury site. Because the magnitude of k_B is a source of considerable debate we ran each simulation at the low end (100 s^{-1}) and high end (6500 s^{-1}) of reported values.[27]

RESULTS

Table 1 summarizes the experimental conditions used in this study. Human whole blood was perfused over fibrillar type I collagen adsorbed to the NO releasing polymer films. Six NO flux conditions ranging from 0.07 to 12 × 10^{-10} mol cm^{-2} min^{-1} were tested at three wall shear rates (200, 500 and 1000 s^{-1}). Computational simulations of NO transport were performed with the same flux and shear rate conditions as the experiments to estimate the near wall NO concentration.

Characterization of NO Polymer

The NO polymer consists of two layers: a NO releasing film containing the NO donor and a top coat that regulates the diffusion of water into the base layer. Polymer solutions were drop coated within a 33 mm × 83 mm incubation chamber. A combination of 5 mL of the NO releasing solution followed by 4 mL of the top coat solution gave a bilayer thickness of 110 μm ± 6 μm. There was an initial transient increase in NO flux over ~15 min, after which, the flux reached a steady state that was maintained for several hours (Fig. 1). Blood flow assays were performed after 1 h of buffer exposure and the duration of the assay was 5 min, so we assumed that the flux was constant during course of the flow assay. The average NO flux of the polymer films ranged from 0.07 to 12 × 10^{-10} mol cm^{-2} min^{-1}, spanning below and above measured fluxes of 0.4–5 × 10^{-10} mol cm^{-2} min^{-1} obtained from endothelial cells within a static environment.[30] Table 2 shows the average NO flux from 1–2 h for each NO wt%. Flow assays were always conducted during this time period. The measured fluxes were assumed to be comparable to NO fluxes in the blood flow assays, and as such, all subsequent results are presented in terms of NO flux.

The Effect of NO Flux on Platelet Aggregation

Platelet aggregate size was influenced by NO flux in whole blood flow assays over collagen-functionalized substrates at 200 and 500 s^{-1} (Fig. 2). At the highest NO flux range (6.8 × 10^{-10} to 12 × 10^{-10} mol cm^{-2} min^{-1}), single platelets adhered on the surface, but no aggregates were observed. At the mid NO flux range (0.40 × 10^{-10} to 2.5 × 10^{-10} mol cm^{-2} min^{-1}), there was a combination of platelet aggregates surrounded by individual

TABLE 1. Experimental conditions and computational results from whole blood flow assays over NO releasing polymer films.

Wall shear rate (s^{-1})	Flux ($\times 10^{-10}$ mol cm^{-2} min^{-1})	Pe*	Effective penetration depth, λ (μm) $k_B = 100$ s^{-1}**	Effective penetration depth, λ (μm) $k_B = 6500$ s^{-1}**	Avg NO conc in PRL (nM) $k_B = 100$ s^{-1}***	Avg NO conc in PRL (nM) $k_B = 6500$ s^{-1}***
200	0.07	19	0	0	3	1
200	0.33	19	1.5	1.5	12	3
200	0.4	19	2.7	1.8	14	4
200	2.5	19	13	4.8	90	24
200	6.8	19	19	6.8	240	65
200	12	19	22	8.4	430	110
500	0.07	48	0	0	2.5	0.67
500	0.33	48	1.5	1.5	12	3
500	0.4	48	2.7	1.8	14	4
500	2.5	48	13	4.8	90	24
500	6.8	48	19	6.8	240	65
500	12	48	22	8.4	430	110
1000	0.07	94	0	0	2.5	0.67
1000	0.33	94	1.5	1.5	12	3
1000	0.4	94	2.7	1.8	14	4
1000	2.5	94	13	4.8	90	24
1000	6.8	94	19	6.8	240	65
1000	12	94	22	8.4	430	110

The NO flux from polymer films was measured experimentally. The effective penetration depth (λ) and the average NO concentration in PRL were calculated from simulations.

* The Pe number is calculated from Suppl. Eq. 14.

** The effective penetration depth was found at $x = 5.5$ mm and was determined to be the depth in which concentration was greater than or equal to 12 and 3 nM for a k_B of 100 and 6500 s^{-1}, respectively. If the concentration of NO was less than these values, it was considered a subthreshold concentration to induce inhibition and is denoted by zero in the table.

*** The average concentration of NO in the PRL was determined over the range of $x = 5$–10 mm and $y = 1$–3 μm.

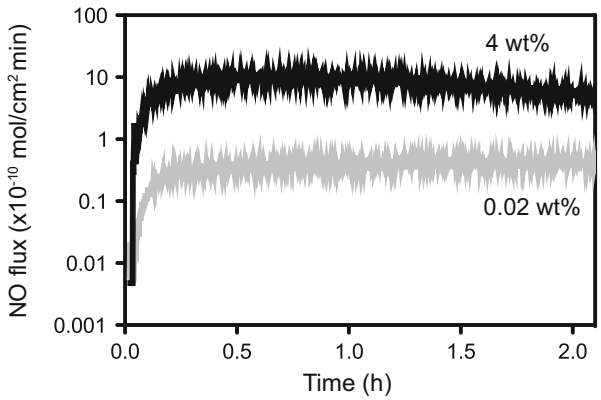

FIGURE 1. Flux of NO from polymer coated glass coverslips loaded with 0.02 or 4 wt% NO donor. These loading represent the minimum and maximum used in the flow assay experiments. The generation NO gas was determined by chemiluminescence.

platelets adhered on the surface. At low surface fluxes (0.07×10^{-10} to 0.33×10^{-10} mol cm^{-2} min^{-1}) and control conditions, the platelets formed larger aggregates. Annexin V was perfused over the surface to measure PS exposure, a marker for platelet activation, following the blood flow assay. All platelet aggregates were PS positive, even at the highest flux. Figure 3 shows representative images at 500 s^{-1}. No axial dependence in platelet accumulation was observed.

TABLE 2. NO flux as a function of loading of NO donor.

NO wt%	NO flux ($\times 10^{-10}$ mol cm^{-2} min^{-1})
0.02	0.07 ± 0.03
0.08	0.33 ± 0.05
0.2	0.40 ± 0.07
0.8	2.5 ± 1.8
2	6.8 ± 2.9
4	12 ± 7.8

The NO donor (DBHD/N_2O_2) was loaded into PVC-DOS-THF polymer solution at various weight percentages to modulate NO flux. The flux was measured by chemiluminescence over 2 h and is reported as the average flux ±standard deviation ($n = 5$) from 15 min to 2 h.

Human whole blood was perfused over the control polymer and compared to OTS modified glass, which was meant to mimic the hydrophobic surface of the polymer. There was no statistical difference in thrombus heights and the size of platelet aggregates between the control polymer and OTS samples (data not shown). Consequently, we concluded that the differences in platelet aggregation obtained on the NO polymer were due to the release of NO, and not any intrinsic surface properties of the polymer top coat.

For each experimental condition, the average platelet aggregate area and average platelet aggregate height were

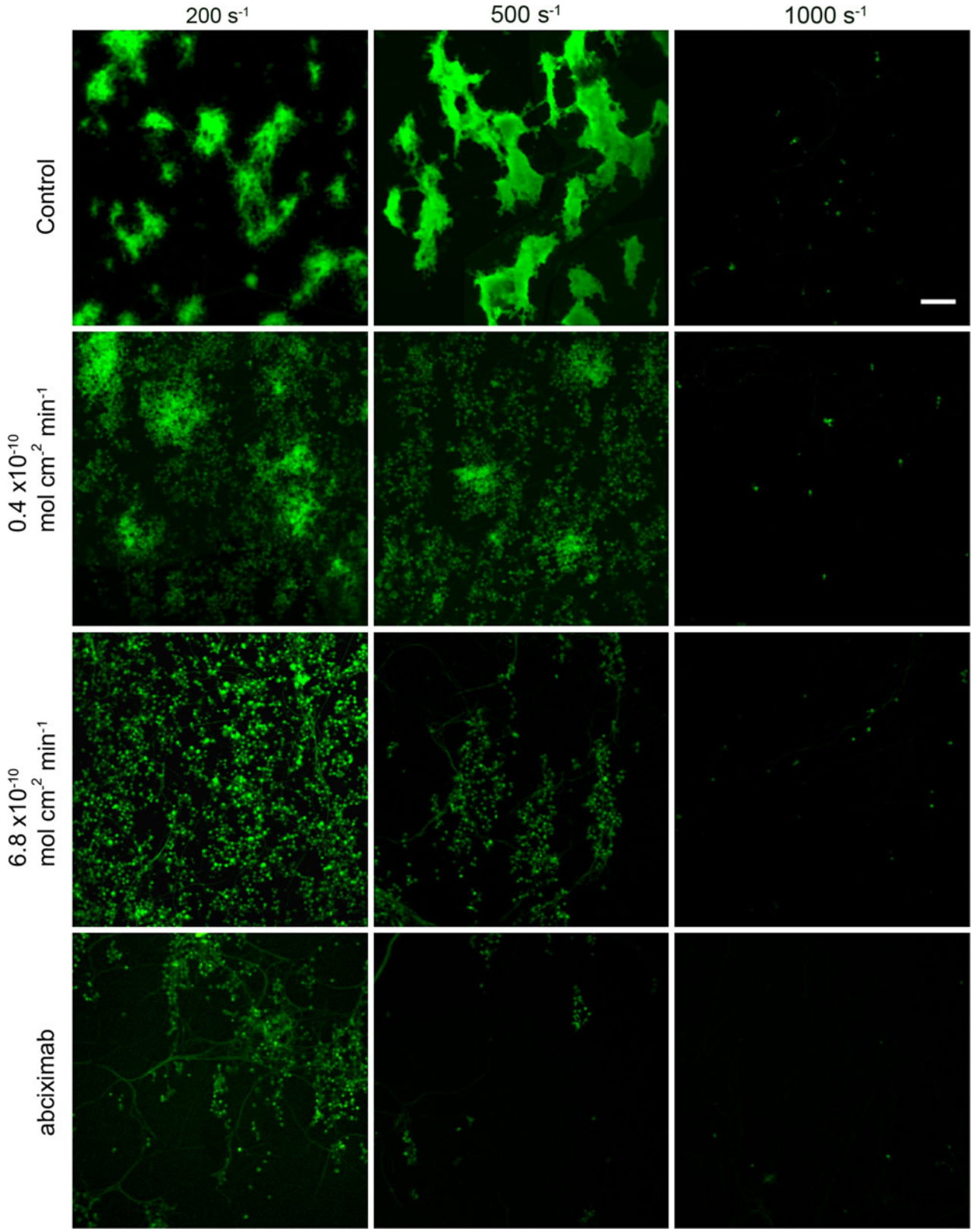

FIGURE 2. Representative images of platelet accumulation on type I fibrillar collagen adsorbed to polymer surfaces at 200, 500 and 1000 s^{-1} at NO wall fluxes of 0.4 × 10^{-10} and 6.8 × 10^{-10} mol cm^{-2} min^{-1}. The negative control is a polymer with no NO donor (control). The positive control is inhibition with abciximab. Platelets are labeled with an anti-CD41 antibody. Scale bar = 25 μm.

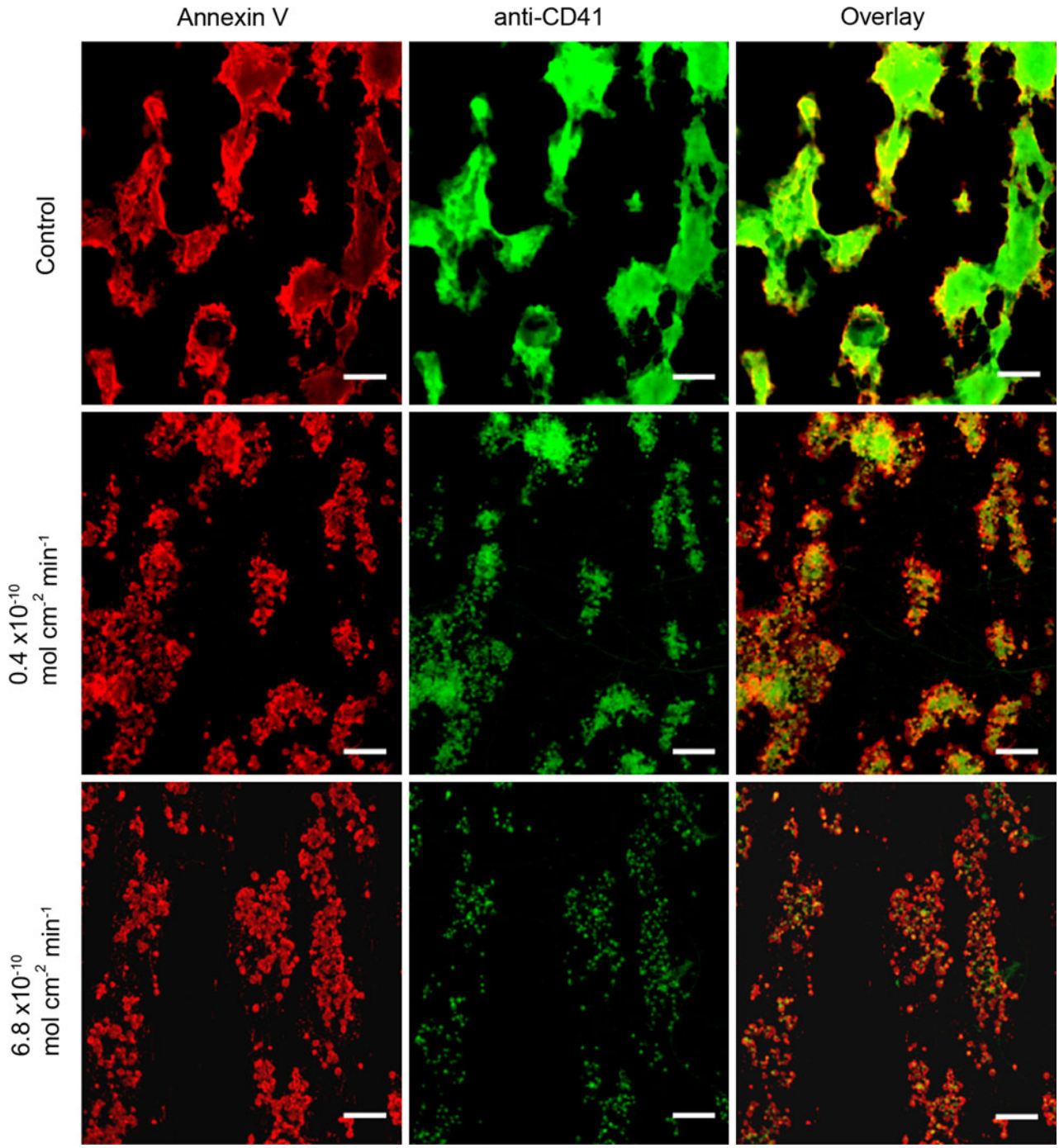

FIGURE 3. Activated platelets adhere to and aggregate on type I fibrillar collagen on NO releasing polymer surfaces at 500 s^{-1}. Annexin V (red) labels PS positive platelets and anti-CD41 (green) labels all platelets. A control, mid range flux (0.4×10^{-10} mol cm^{-2} min^{-1}) and high range flux (6.8×10^{-10} mol cm^{-2} min^{-1}) are shown. Scale bar = 25 μm.

measured. There were ~200 aggregates measured in each assay. Platelet aggregates were categorized as less than 20 μm^2, between 20 and 1000 μm^2, and greater than 1000 μm^2. There was a similar frequency of platelet aggregates less than 20 μm^2 and between 20 and 1000 μm^2 for all conditions tested. However, there was a significant difference ($p < 0.05$) between experimental conditions when comparing platelet aggregates greater than 1000 μm^2 at a flux of 2.5×10^{-10} mol cm^{-2} min^{-1} at 200 and 500 s^{-1} (Fig. 4a–c). A flux of 0.07 mol cm^{-2} min^{-1} resulted in no differences ($p > 0.05$) in height compared to the control sample at all shear rates.

At 200 and 500 s^{-1}, an effect was observed at a flux of 0.33×10^{-10} mol cm^{-2} min^{-1}. However at 1000 s^{-1}, the NO flux did not have an effect, even at the highest flux of 12×10^{-10} mol cm^{-2} min^{-1} (Fig. 4d).

To determine the maximum inhibition possible, each condition was compared to an assay ran in the presence of abciximab, an $\alpha_{IIb}\beta_3$ antagonist, that completely inhibits platelet aggregation. Experiments done with abciximab revealed an average platelet height of less than 1 μm and an average platelet area of 5–10 μm^2. Any fluxes that lead to platelet accumulation that was statistically indistinguishable ($p > 0.05$) from the abciximab condition were considered to have achieved maximal inhibition. At 200 and 500 s^{-1}, the NO flux that resulted in maximum inhibition with respect to platelet aggregate height and area was 2.5×10^{-10} mol cm^{-2} min^{-1}. Thus the dynamic range of NO fluxes that are capable of inhibiting platelet aggregation as measured by height in this assay are between 0.33×10^{-10} and 2.5×10^{-10} mol cm^{-2} min^{-1}.

NO Concentration at the Wall and Within the Platelet Rich Layer (PRL)

In the flow assay experiments we varied the NO flux and the wall shear rate. We developed a computational model to predict the concentration distribution of NO under these experimental conditions (Fig. 5a). The model was performed using first order rate constants of NO elimination by hemoglobin in RBC (k_B) of 100 and 6500 s^{-1}. The average NO concentration within the PRL over the collagen injury is reported in Table 1. The minimum flux required to see reduced platelet

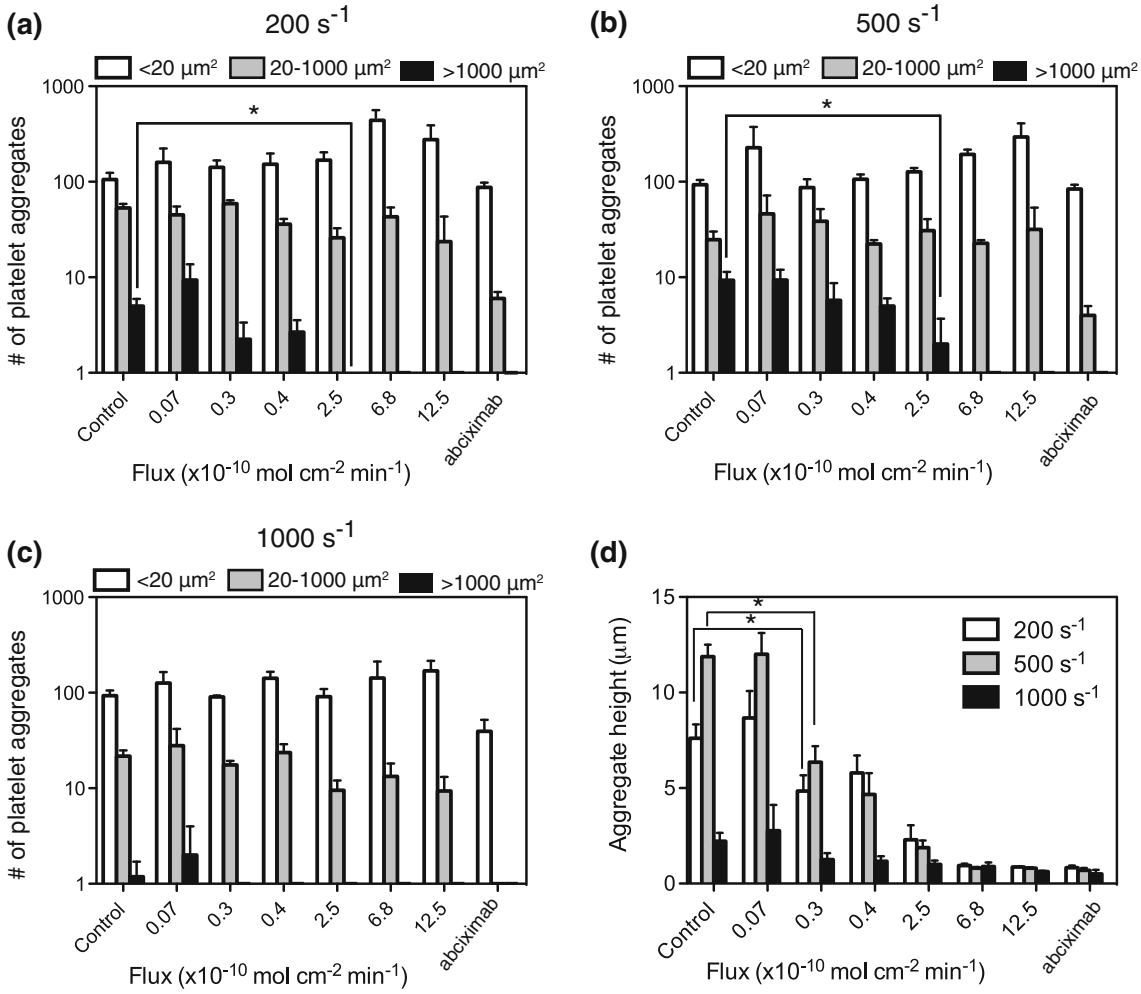

FIGURE 4. Platelet aggregates decrease in size with increasing NO flux. Platelet aggregate areas are categorized by size; <20 μm^2, 20–1000 and >1000 μm^2 for each NO flux at (a) 200, (b) 500 and (c) 1000 s^{-1}. (d) Platelet aggregate heights are shown at the same conditions as aggregate areas (n = 3–4 donors for all conditions). All conditions are compared to abciximab, representative of maximal platelet aggregation inhibition. Error bars indicate standard error of the mean across donors at each condition. Significant differences ($p < 0.05$) are denoted by asterisk.

aggregation was 0.33×10^{-10} mol cm^{-2} min^{-1}, corresponding to a NO concentration of 3 and 12 nM for 6500 and 100 s^{-1}. A flux of 2.5×10^{-10} mol cm^{-2} min^{-1} was required to completely inhibit aggregation and correlated to a NO concentration of 24 and 90 nM in the PRL at k_B of 6500 and 100 s^{-1}.

The penetration and accumulation of NO into the channel can be characterized by the relative rates of transport and elimination mechanisms. The Peclet (Pe) number represents the rate of convection to the rate of diffusion. In the experiment, Pe number ranged from 19 to 94 over shear rates of 200–1000 s^{-1} indicating

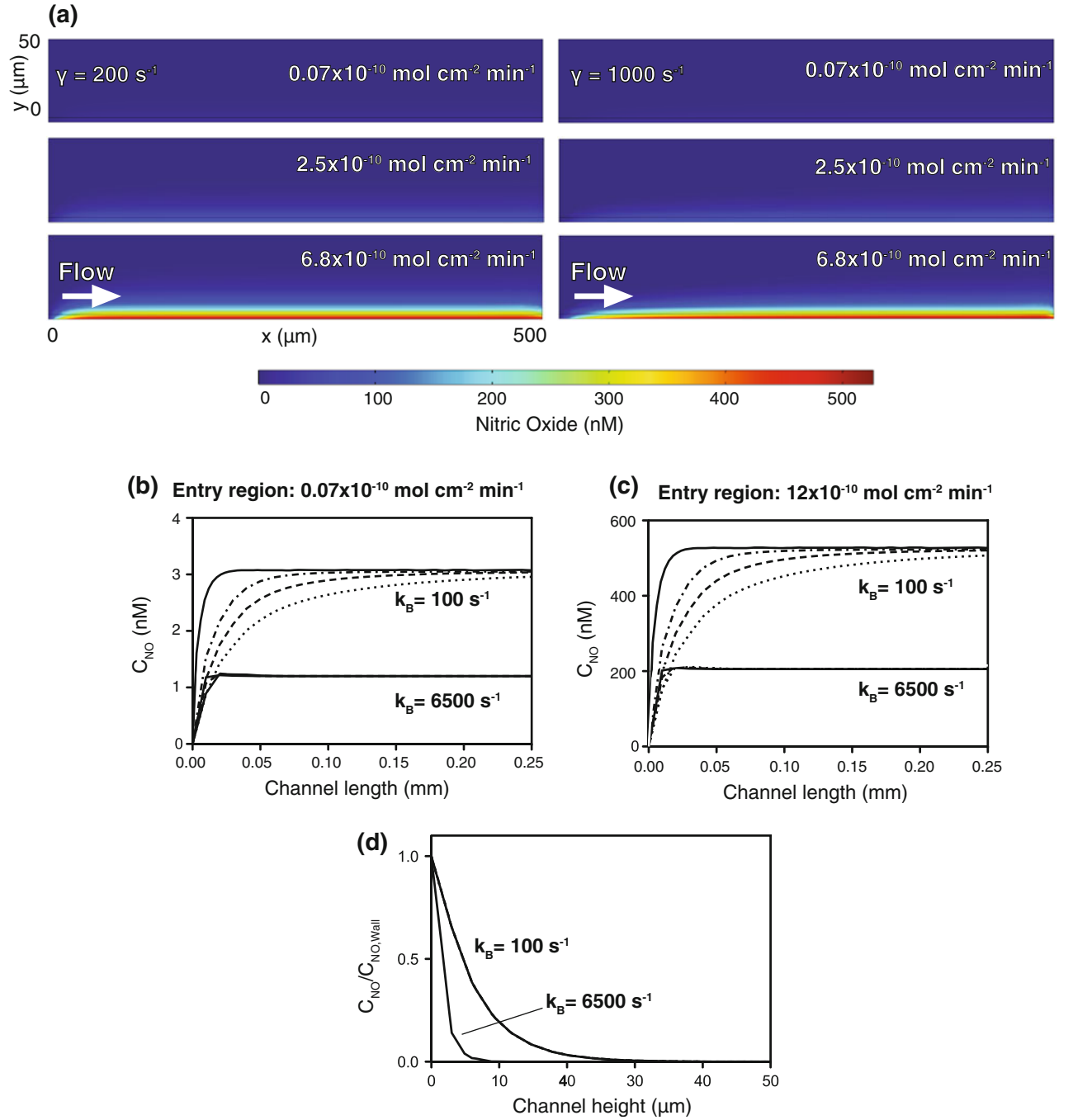

FIGURE 5. (a) NO distribution within the entry region of the channel as function of NO flux at shear rates of 200 and 1000 s^{-1} at k_B = 100 s^{-1}. NO wall concentrations in the entry region for fluxes of 0.07×10^{-10} mol cm^{-2} min^{-1} (b) and 12×10^{-10} mol cm^{-2} min^{-1} (c), at shear rates of 200 s^{-1} (dotted dashed line), 500 s^{-1} (dashed line) and 1000 s^{-1} (dotted line). The solid line indicates static conditions. (d) Normalized NO concentration into the lumen of the channel (perpendicular to flow) at x = 5.5 mm as a function first order rate constant for elimination in the blood (k_B). The profile in the height direction is effectively independent of shear rate.

convective transport dominates outside the momentum boundary layer. The first Damkoher number, Da_I, compares the NO elimination by reaction with oxygen to diffusion in the PRL ($Da_I = k_{O2}J_{NO}\delta^3/D_{NO}^3$) and was found to range from 10^{-8} to 10^{-6}. This means that diffusion from the wall to the edge of the PRL was much faster than elimination by oxygen. The second Damkohler number, Da_{II}, which is applicable in the bulk of fluid where the local Pe number is greater than one (domain 1, Suppl. Fig. 2), represents the rate of elimination of NO by reaction with blood compared to the rate of mass transfer (k_g) from the wall into the bulk ($Da_{II} = k_B C_{NO,wall} h/k_g$). For all fluxes and wall shear rates, Da_{II} was 11 for $k_B = 100\ s^{-1}$ and 330 for $6500\ s^{-1}$, indicating that the reaction with blood in the bulk was faster than the mass transfer. The NO concentrations in the PRL at each flux were a weak function of k_B (Table 1). The shear rate had a slight effect in the entry region of the channel at a k_B of $100\ s^{-1}$ (Fig. 5b–c). At a k_B of $6500\ s^{-1}$, all shear rates and the static condition were identical (Fig. 5b–c). Outside of the entry region, the normalized NO concentration was independent of wall shear rate (Fig. 5d). As expected, the penetration into the lumen of the channel was greater for $k_B = 100\ s^{-1}$ than for $k_B = 6500\ s^{-1}$ (Table 1, Fig. 5d).

The fidelity of the computational grid and solver were validated by a comparison to the analytical solution for the 1D diffusion-reaction conservation of mass with a constant wall flux BC (Eqs. S17–S18, Supplementary Material). The NO concentration distribution in the direction perpendicular to the flow (y-direction) was calculated at four different points in the y direction (1, 5, 10 and 25 μm). Less than a 5% difference was found between the analytical solution and corresponding computational solution at each shear rate.

Injury Model

We extended the model to simulate how the loss of endothelial cells at the site of an injury affects the NO transport surrounding the injury. An injury size of 100 μm was investigated, starting in a fully developed region (~1 mm downstream of the inlet) (Fig. 6). All simulation conditions were identical to those described above, except within the injury zone the bottom ($y = -h/2$) boundary condition was set to a zero flux. Concentration profiles for each injury size were assessed at low and high NO fluxes ($J_{NO,low} = 0.07 \times 10^{-10}$ mol cm^{-2} min^{-1}, $J_{NO,high} = 12 \times 10^{-10}$ mol cm^{-2} min^{-1}) and low and high wall shear rates ($\gamma_{low} = 200\ s^{-1}$, $\gamma_{high} = 1000\ s^{-1}$). At a k_B of $100\ s^{-1}$, the rate of the NO decay over the injury was determined by the shear rate and NO flux. As expected, a higher flux led to a higher residual concentration of NO in the injury zone. A higher shear rate also led to a higher residual concentration, presumably due to enhanced axial convection. At a k_B of $6500\ s^{-1}$ for both shear rates and fluxes, the NO concentration dropped to zero within 5 μm of the edge of the injury zone.

DISCUSSION

The purpose of this study was to determine the transport limitations of NO mediated inhibition of platelets over a physiologic range of shear rates. We integrated a NO releasing polymer into a microfluidic flow assay to determine the dynamic range of NO fluxes that would inhibit collagen mediated platelet aggregation. A computational model of NO transport was developed to estimate the NO concentration profiles under the experimental conditions, and to extrapolate experimental results to the case where an injury would cause a disruption of the endothelium.

The dynamic range NO fluxes affecting platelet aggregation in our flow assay was 0.33×10^{-10} to 2.5×10^{-10} mol cm^{-2} min^{-1}. A flux of 0.33×10^{-10} mol cm^{-2} min^{-1} measurably inhibited platelet aggregation at wall shear rates of 200 and $500\ s^{-1}$. A computational model of the experiments estimates that this flux results in an average NO concentration of 3–12 nM for rate constants of 100 and $6500\ s^{-1}$, respectively, independent of shear rate. The NO flux required to completely inhibit platelet aggregation was 2.5×10^{-10} mol cm^{-2} min^{-1}, corresponding to 24–90 nM within the PRL at 200 and $500\ s^{-1}$. These concentrations are within range of measured arterial NO concentrations (2 nM[16]–1 μM[15]).

This is first study to quantify the effect NO wall flux on platelet adhesion and aggregation over a range of shear rates in whole blood. Roberts *et al.*[21] added a NO donor exogenously and mixed homogenously throughout the blood, which does not capture the spatial dependence of NO release from the vessel wall. De Graaf *et al.*[7] released NO from the wall *via* a saline solution at 3.0% NO, but the resulting concentration of NO was not reported. Ramamurhti and Lewis introduced gaseous NO into a flow assay through a permeable membrane and estimated that a NO concentration of 0.09 nM completely inhibited platelet adhesion and aggregation on collagen.[20] This concentration is more than three orders-of-magnitude lower than the critical concentration found in this study. The likely explanation for this difference is their use of a suspension of washed platelets compared to our whole blood experiment. In the absence of RBC, the near-wall density of platelets would be significantly reduced and there would be no elimination of NO *via* hemoglobin.

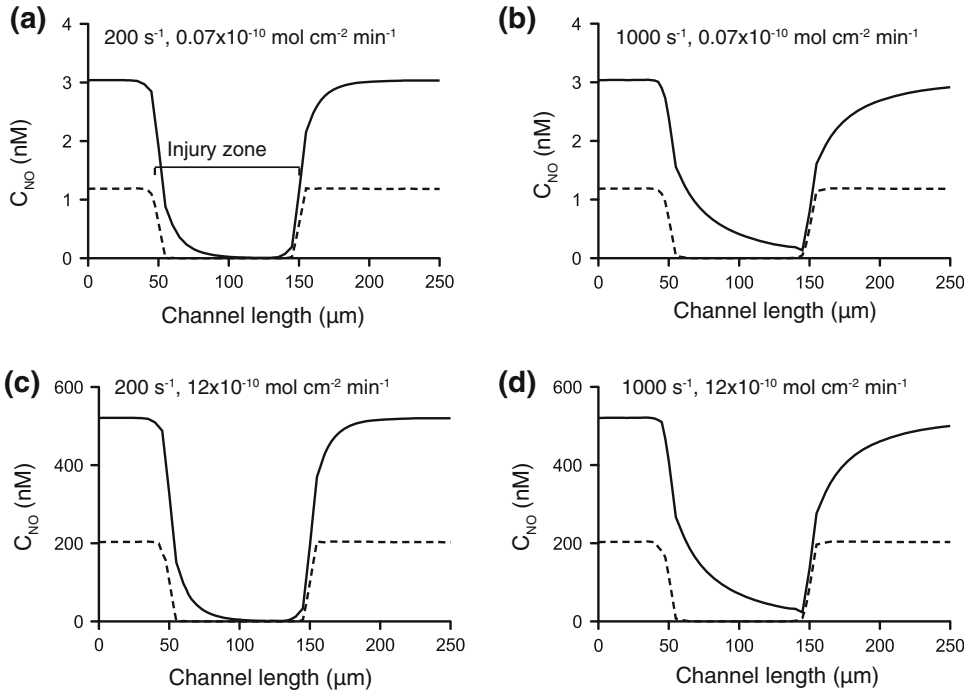

FIGURE 6. NO wall concentration profiles along an simulated injury of length of 100 μm. The injury zone, which starts at $x = 50$ μm, simulates the loss of NO flux due to the absence of endothelial cells. Concentration profiles for each injury size at a flux of 0.07 × 10^{-10} mol cm^{-2} min^{-1} at (a) 200 s^{-1} and (b) 1000 s^{-1} and at a flux of 12 × 10^{-10} mol cm^{-2} min^{-1} at (c) 200 s^{-1} and (d) 1000 s^{-1}. For all graphs, black denotes a k_B of 100 s^{-1} and dashed shows a k_B of 6500 s^{-1}.

The same NO flux was required to achieve complete aggregation inhibition at 200 and 500 s^{-1}. The mass transfer from the wall is weakly related to shear rate ($\gamma^{1/3}$), so it is not surprising that there was no measurable difference between the two shear rates. These results are consistent with the prediction of the computational model, as all effective penetration depths were identical at both shear rates except for at 0.33 × 10^{-10} mol cm^{-2} min^{-1}, where the penetration depth was reduced at 500 s^{-1} yet still was greater than the PRL thickness (~3 μm).

In all cases, annexin V labeling indicated that the platelets exposed PS, a marker for GPVI outside-in signaling.[23] This result is in agreement with previous studies showing that GPVI is constitutively active even in the presence of NO. Platelets under flow can still bind to collagen *via* their GPVI receptor.[22] Integrins $\alpha_2\beta_1$ and $\alpha_{IIb}\beta_3$, known to sustain stable adhesion, aggregation and spreading,[21] are less active in the presence of the NO.[22] Diminished $\alpha_2\beta_1$ and $\alpha_{IIb}\beta_3$ dimerization could explain the reduction in platelet aggregate height and area in flow assays.

Our computational model of NO transport of the experimental conditions in an *in vitro* flow assay showed that NO penetration into the lumen was transport limited. The primary determinant of NO concentration in the lumen was the first order rate constant with blood. These prediction are similar to previous models.[4,29] For example, Vaughn *et al.* used a NO flux of 3.2 × 10^{-10} mol cm^{-2} min^{-1}, slightly greater than our critical value 2.5 × 10^{-10} mol cm^{-2} min^{-1}, and found NO concentration to vary from 25 to 100 nM with rate constants of 230,000–150 s^{-1}. A rate constant of 15 s^{-1}, much lower than most reported values, was required to obtain a concentration of 250 nM, the dissociation constant of sGC.[26] Subsequent studies have suggested that the sCG dissociation may be closer to 1 nM,[2] which is similar to the effective concentration found in this study (3–12 nM in PRL). The majority of recent studies on NO elimination in the presence of RBC report reaction rate constants in the range 1000–6500 s^{-1},[27,28] leading us to believe that the lower end of our concentration range (3 nM) is more representative. Smith *et al.* reported that the convective transport was insensitive to NO scavenging by hemoglobin at a NO flux of 0.20 × 10^{-10} mol cm^{-2} min^{-1}, slightly less than the effective flux (0.33 × 10^{-10} mol cm^{-2} min^{-1}) found in this study, because the NO-hemoglobin binding rate was slow relative to the convection. Differences between our models are attributed to their low reaction rate constant (30 s^{-1}).[25]

There are a few notable limitations of the experimental and computational models. First, whole blood in the experiments was collected into the thrombin inhibitor PPACK. Consequently, the effect of NO on

platelet aggregation was primarily inhibiting ADP and thromboxane A2 mediated activation. In the computational model, blood was considered to be a Newtonian fluid because it was perfused at shear rates greater than or equal to 200 s^{-1}. But the model does not take into account the particulate nature of the blood, which will likely influence the solute transport by enhanced mixing.[17] The only source of NO in the model is the NO releasing polymer on the bottom of the channel. However, RBC and platelets are other potential sources of NO.[6,9] The channel height used in the experiments is typical of venules and arterioles, and therefore our results may be limited to small vessels. Additionally, the platelet aggregates were only measured by height and area measurements. Quantifying the volume of the platelet aggregates would better account for the variable shape of different deposits.

An injury model was presented to estimate the bioavailability of NO within the vicinity of an injury as various sized sections of NO flux were removed to mimic loss of endothelial cells. It was shown that the severity of the injury is related to the magnitude of the flux and shear rate at a k_B of 100 s^{-1}. An increase of shear rate was found to prolong the NO effect over the injury zone. At a k_B of 6500 s^{-1}, the shear rate did not affect the concentration profile, and virtually no NO was present in the injury zone. These results suggest that the ability of NO to regulate thrombus growth may be limited to the periphery of an injury where NO concentrations are within their effective range. The injury model does not take into account possible upregulation of NO sources, eNOS and iNOS,[12] or negative feedback mechanisms[19] within an injury zone, which may be important *in vivo*.

CONCLUSIONS

We have developed an assay that decouples the effect of shear rate and NO flux on platelet function by incorporating NO releasing polymers within a microfluidic vascular injury model. To our knowledge, no previous platelet function study under flow has been done at a defined wall flux of NO with whole blood. It was shown that NO begins to have an effect on collagen mediated platelet aggregation at an NO flux of 0.33×10^{-10} mol cm^{-2} min^{-1} and complete abrogation of platelet aggregation was attained at a NO flux of 2.5×10^{-10} mol cm^{-2} min^{-1} at 200 and 500 s^{-1}. A computational model was used to estimate transport limitations of NO and estimate NO concentrations within the experiment. A near-wall NO concentration of 3–90 nM was predicted to be the dynamic range over which platelet aggregation was inhibited. NO concentration of >100 nM completely abrogated platelet aggregation. The penetration depth and local NO concentration were found to be transport limited, with the rate of elimination of NO in whole blood to be the primary determinant of NO distribution in the lumen.

ELECTRONIC SUPPLEMENTARY MATERIAL

The online version of this article (doi:10.1007/s10439-013-0803-9) contains supplementary material, which is available to authorized users.

ACKNOWLEDGMENTS

This work was supported by a Scientist Development Grant (K.B.N.) from the American Heart Association, the Colorado Office of Economic Development and International Trade, and the Boettcher Foundation's Webb-Waring Biomedical Research Award (K.B.N and M.M.R).

REFERENCES

[1]Antl, M., M. L. von Bruhl, C. Eiglsperger, M. Werner, I. Konrad, T. Kocher, M. Wilm, F. Hofmann, S. Massberg, and J. Schlossmann. IRAG mediates NO/cGMP-dependent inhibition of platelet aggregation and thrombus formation. *Blood* 109:552–559, 2007.

[2]Ballou, D. P., Y. Zhao, P. E. Brandish, and M. A. Marletta. Revisiting the kinetics of nitric oxide (NO) binding to soluble guanylate cyclase: the simple NO-binding model is incorrect. *Proc. Natl. Acad. Sci.* 99:12097–12101, 2002.

[3]Batchelor, M. M., S. L. Reoma, P. S. Fleser, V. K. Nuthakki, R. E. Callahan, C. J. Shanley, J. K. Politis, J. Elmore, S. I. Merz, M. E. Meyerhoff. More lipophilic dialkyldiamine-based diazeniumdiolates: synthesis, characterization, and application in preparing thromboresistant nitric oxide release polymeric coatings. *J. Med. Chem.* 46:5153–5161, 2003.

[4]Butler, A. R., I. L. Megson, and P. G. Wright. Diffusion of nitric oxide and scavenging by blood in the vasculature. *Biochim. Biophys. Acta* 1425:168–176, 1998.

[5]Condorelli, P., and S. C. George. In vivo control of soluble guanylate cyclase activation by nitric oxide: a kinetic analysis. *Biophys. J.* 80:2110–2119, 2001.

[6]Cortese-Krott, M. M., A. Rodriguez-Mateos, R. Sansone, G. G. C. Kuhnle, S. Thasian-Sivarajah, T. Krenz, P. Horn, C. Krisp, D. Wolters, C. Heiss, K. D. Kroncke, N. Hogg, M. Feelisch, and M. Kelm. Human red blood cells at work: identification and visualization of erythrocytic eNOS activity in health and disease. *Blood* 120:4229–4237, 2012.

[7]de Graaf, J. C., J. D. Banga, S. Moncada, R. M. Palmer, P. G. de Groot, and J. J. Sixma. Nitric oxide functions as

an inhibitor of platelet adhesion under flow conditions. *Circulation* 85:2284–2290, 1992.
[8]Fadel, A. A., K. A. Barbee, and D. Jaron. A computational model of nitric oxide production and transport in a parallel plate flow chamber. *Ann. Biomed. Eng*. 37:943–954, 2009.
[9]Freedman, J. E., J. Loscalzo, M. R. Barnard, C. Alpert, J. F. Keaney, and A. D. Michelson. Nitric oxide released from activated platelets inhibits platelet recruitment. *J. Clin. Invest*. 100:350–356, 1997.
[10]Hansen, R. R., A. A. Tipnis, T. C. White-Adams, J. A. Di Paola, and K. B. Neeves. Characterization of collagen thin films for von Willebrand factor binding and platelet adhesion. *Langmuir* 27:13648–13658, 2011.
[11]Kanai, A. J., H. C. Strauss, G. A. Truskey, A. L. Crews, S. Grunfeld, and T. Malinski. Shear stress induces ATP-independent transient nitric oxide release from vascular endothelial cells, measured directly with a porphyrinic microsensor. *Circ. Res*. 77:284–293, 1995.
[12]Kibbe, M., T. Billiar, and E. Tzeng. Inducible nitric oxide synthase and vascular injury. *Cardiovasc. Res*. 43:650–657, 1999.
[13]Kim, S., P. K. Ong, O. Yalcin, M. Intaglietta, and P. C. Johnson. The cell-free layer in microvascular blood flow. *Biorheology* 46:181–189, 2009.
[14]Kuchan, M. J., and J. A. Frangos. Role of calcium and calmodulin in flow-induced nitric oxide production in endothelial cells. *Am. J. Physiol*. 266:C628–C636, 1994.
[15]Malinski, T., Z. Taha, S. Grunfeld, S. Patton, M. Kapturczak, and P. Tomboulian. Diffusion of nitric oxide in the aorta wall monitored in situ by porphyrinic microsensors. *Biochem. Biophys. Res. Commun*. 193:1076–1082, 1993.
[16]Mochizuki, S., T. Miyasaka, M. Goto, Y. Ogasawara, T. Yada, M. Akiyama, Y. Neishi, T. Toyoda, J. Tomita, Y. Koyama, K. Tsujioka, F. Kajiya, T. Akasaka, and K. Yoshida. Measurement of acetylcholine-induced endothelium-derived nitric oxide in aorta using a newly developed catheter-type nitric oxide sensor. *Biochem. Biophys. Res. Commun*. 306:505–508, 2003.
[17]Nanne, E. E., C. P. Aucoin, and E. F. Leonard. Shear rate and hematocrit effects on the apparent diffusivity of urea in suspensions of bovine erythrocytes. *ASAIO J*. 56:151–156, 2010.
[18]Naseem, K. M., and W. Roberts. Nitric oxide at a glance. *Platelets* 22:148–152, 2011.
[19]Plata, A. M., S. J. Sherwin, and R. Krams. Endothelial nitric oxide production and transport in flow chambers: the importance of convection. *Ann. Biomed. Eng*. 38:2805–2816, 2010.
[20]Ramamurthi, A., and R. S. Lewis. Influence of agonist, shear rate, and perfusion time on nitric oxide inhibition of platelet deposition. *Ann. Biomed. Eng*. 28:174–181, 2000.
[21]Roberts, W., A. Michno, A. Aburima, and K. M. Naseem. Nitric oxide inhibits von Willebrand factor-mediated platelet adhesion and spreading through regulation of integrin Î ± IIbÎ²3and myosin light chain. *J. Thromb. Haemost*. 7:2106–2115, 2009.
[22]Roberts, W., R. Riba, S. Homer-Vanniasinkam, R. W. Farndale, and K. M. Naseem. Nitric oxide specifically inhibits integrin-mediated platelet adhesion and spreading on collagen. *J. Thromb. Haemost*. 6:2175–2185, 2008.
[23]Siljander, P., R. W. Farndale, M. A. Feijge, P. Comfurius, S. Kos, E. M. Bevers, and J. W. Heemskerk. Platelet adhesion enhances the glycoprotein VI-dependent procoagulant response: involvement of p38 MAP kinase and calpain. *Arterioscler. Thromb. Vasc. Biol*. 21:618–627, 2001.
[24]Skrzypchak, A. M., N. G. Lafayette, R. H. Bartlett, Z. Zhou, M. C. Frost, M. E. Meyerhoff, M. M. Reynolds, and G. M. Annich. Effect of varying nitric oxide release to prevent platelet consumption and preserve platelet function in an in vivo model of extracorporeal circulation. *Perfusion* 22:193–200, 2007.
[25]Smith, K. M., L. C. Moore, and H. E. Layton. Advective transport of nitric oxide in a mathematical model of the afferent arteriole. *Am. J. Physiol. Renal Physiol*. 284:F1080–F1096, 2003.
[26]Stone, J. R., and M. A. Marletta. Spectral and kinetic studies on the activation of soluble guanylate cyclase by nitric oxide. *Biochemistry* 35:1093–1099, 1996.
[27]Tsoukias, N. M. Nitric oxide bioavailability in the microcirculation: insights from mathematical models. *Microcirculation* 15:813–834, 2008.
[28]Tsoukias, N. M., and A. S. Popel. Erythrocyte consumption of nitric oxide in presence and absence of plasma-based hemoglobin. *AJP Heart Circ. Physiol*. 282:H2265–H2277, 2002.
[29]Vaughn, M. W., L. Kuo, and J. C. Liao. Effective diffusion distance of nitric oxide in the microcirculation. *Am. J. Physiol*. 274:H1705–H1714, 1998.
[30]Vaughn, M. W., L. Kuo, and J. C. Liao. Estimation of nitric oxide production and reaction rates in tissue by use of a mathematical model. *Am. J. Physiol*. 274:H2163–H2176, 1998.
[31]Wasserman, S. R., Y. T. Tao, and G. M. Whitesides. Structure and reactivity of alkylsiloxane monolayers formed by reaction of alkyltrichlorosilanes on silicon substrates. *Langmuir* 5:1074–1087, 1989.